The La Madera Travertines, Rio Ojo Caliente, northern New Mexico: Investigating the linked system of CO_2-rich springs and travertines as neotectonic and paleoclimate indicators

Laura Crossey, Karl E. Karlstrom, Dennis L. Newell, Ara Kooser, and April Tafoya, 2011, pp. 301-316

in:

Geology of the Tusas Mountains and Ojo Caliente, Author Koning, Daniel J.; Karlstrom, Karl E.; Kelley, Shari A.; Lueth, Virgil W.; Aby, Scott B., New Mexico Geological Society 62nd Annual Fall Field Conference Guidebook, 418 p.

This page is intentionally left blank to maintain order of facing pages.

THE LA MADERA TRAVERTINES, RIO OJO CALIENTE, NORTHERN NEW MEXICO: INVESTIGATING THE LINKED SYSTEM OF CO_2-RICH SPRINGS AND TRAVERTINES AS NEOTECTONIC AND PALEOCLIMATE INDICATORS

LAURA J. CROSSEY[1], KARL E. KARLSTROM[1], DENNIS L. NEWELL[2], ARA KOOSER[1], AND APRIL TAFOYA[1]
[1]Department of Earth and Planetary Science, University of New Mexico, Albuquerque, NM 87131; lcrossey@unm.edu
[2]Los Alamos National Laboratory, Earth and Environmental Science Division (EES-14), MS J966, Los Alamos, NM 87545;

Abstract—The La Madera travertine and CO_2-rich spring system of northern New Mexico provides a linked data set to examine neotectonics and mantle-to-surface fluid interconnections in the area of intersection of the Rio Grande rift and Jemez lineament. Water chemistry modeling shows that most of the CO_2 is endogenic (derived from deep geologic sources), with subordinate amounts from dissolution of carbonate and from organic sources. Spring waters are high in arsenic, salts, and metals that mix with and detract from water quality in the regional aquifers, potentially including the Buckman wells near Santa Fe. $^3He/^4He$ data from CO_2-rich hot and cool springs have values ranging from 6.16 to 0.09 R_A (77 to 1% mantle helium), with highest values in the Valles caldera, approaching MORB values (8 R_A). Mantle degassing is interpreted as a neotectonic signal of active upwelling of asthenospheric mantle beneath the Jemez low seismic velocity mantle anomaly. These CO_2 vents align along the NE- and N-trending, tectonically active, extensional faults and fault jogs that parallel the Jemez lineament. The regional continuity and neotectonic activity along these structures suggest an active Embudo-Jemez transfer zone that extends through the Albuquerque, Española, and San Luis basins. Endogenic fluid flux along this zone takes place in fault systems and is driven by geothermal pressure gradients. Travertines are deposited by CO_2-rich waters that ascend along faults and hence they provide a record of past and ongoing mantle ^3He and CO_2 degassing. U-series dating so far, with ages back to >500 ka, suggests an episodicity in deposition of large volumes of travertine that may reflect regional wet periods with high groundwater head. Abundant deposition in the 200-100 ka range may provide a local record of the transition from the penultimate glaciation (135 ka) to the ensuing interglacial (125 ka) that is documented globally by the transition from marine oxygen isotope stage 6 to oxygen isotope stage 5. U-series dates on travertine-cemented terraces also provide precise river incision rates that vary from 100-300 m/Ma indicating differential landscape evolution across the region influenced by both regional tectonism and climate change.

OVERVIEW

Extensive travertine deposits that we refer to as the La Madera travertines occur along the Rio Ojo Caliente near La Madera, NM (Fig.1), and the springs in the region continue to deposit travertine today. These travertines are datable with high-precision uranium-series methods now capable of obtaining age uncertainties of less than 1%. Thus, the travertines preserved in this landscape provide a potentially powerful tool for understanding paleohydrology (Goff and Shevenell, 1987), paleoclimate (Winograd et al., 1992), and differential river incision (Pederson et al., 2002). Travertine deposits precipitate from CO_2-rich groundwaters issuing from springs aligned along the normal fault at the base of La Madera Mountains (Fig. 2). Travertine forms several modern and extinct spring-mound deposits. Large platforms of flowstone are at a similar elevation to mapped fluvial terrace gravels (Newell et al., 2004), and locally cement fluvial terrace gravels of the Rio Ojo Caliente (Koning et al., 2011). Here we report spring water geochemistry in the La Madera area, discuss travertine formation, report ages of travertines in the La Madera area, and compare this occurrence to other regional travertines and CO_2-rich springs in northern New Mexico.

TRAVERTINE AND TRAVERTINE FORMATION

The term travertine (originally Tivertino, tiburtinus and travertino, among others) has its origin from the Roman location of Tivoli, a town east of Rome where extensive quarries, still active today, are found. Travertine exhibits striking banding, and can be translucent with spectacular botryoidal fabrics. It has been found in cultural artifacts (travertine pendants in New Mexico; Zeigler et al., 2011); it also served as the source stone for Canopic jars in early Egyptian usage. Travertine is used extensively as architectural stone, and many classic Roman buildings (the Pantheon and Coliseum, for example) are built from travertine. In New Mexico, active quarries east of Belen have supplied stone for the construction of the State Capital building and buildings at the University of New Mexico. Many geologic definitions of travertine may be found in the literature. Excellent summaries of travertines are presented by Pentecost (2005) and Alonso-Zarza and Tanner (2010a,b). We follow the inclusive definition of Pentecost (2005, p. 2):

> A chemically-precipitated continental limestone formed around seepages, springs and along streams and rivers, occasionally in lakes and consisting of calcite or aragonite, of low to moderate intercrystalline porosity and often high mouldic or framework porosity within a vadose or occasionally shallow phreatic environment. Precipitation results primarily through the transfer (evasion or invasion) of carbon dioxide from or to a groundwater source leading to calcium carbonate supersaturation, with nucleation/crystal growth occurring upon a submerged surface.

While unwieldy, this definition allows for broad application to modern and ancient deposits. Note that calcretes and speleothems

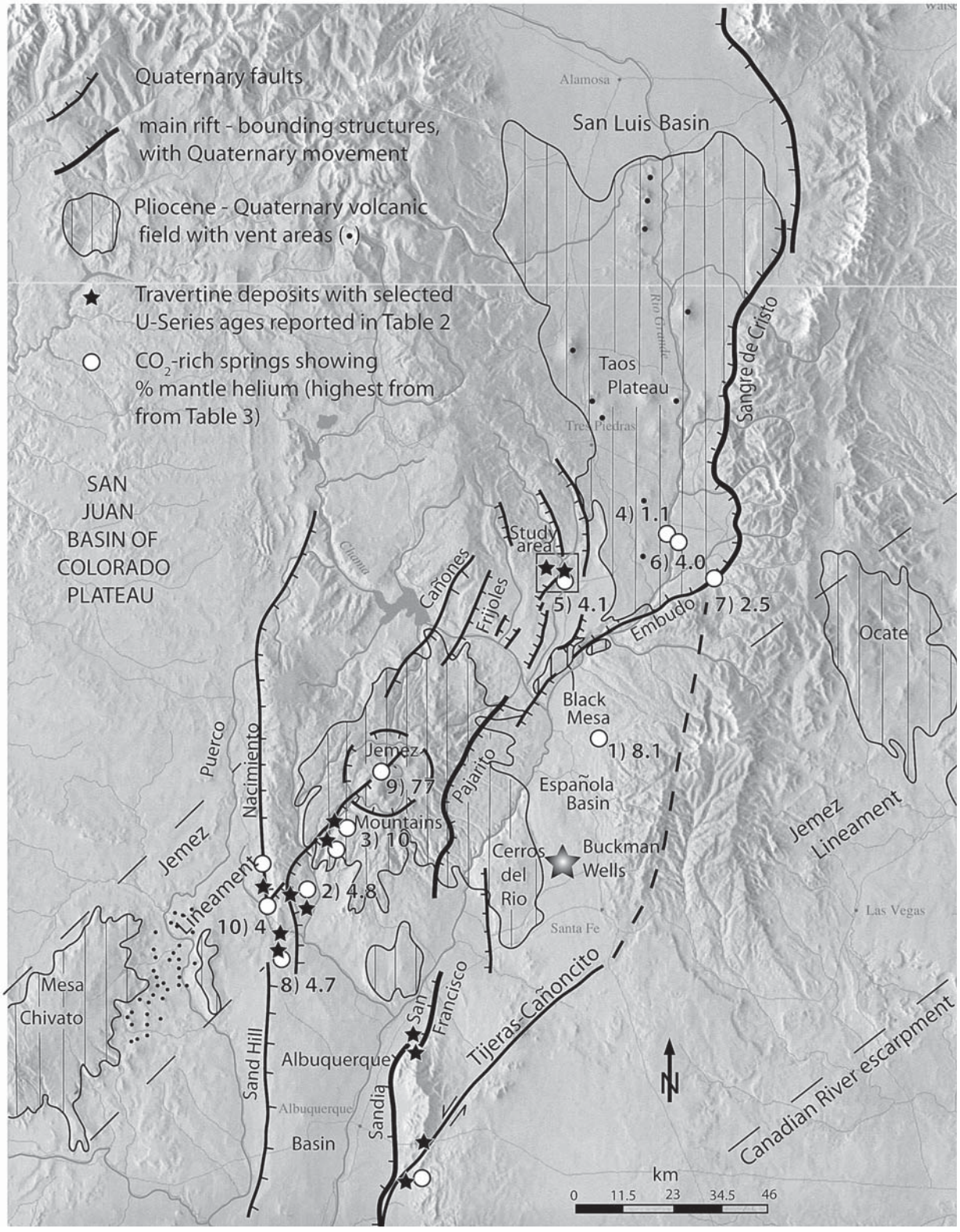

FIGURE 1. Tectonic map of the Embudo- Jemez transfer zone formed at the intersection of the Rio Grande rift and Jemez lineament (map modified from Newell et al., 2004). Neotectonic features of this area include: Quaternary extensional and transtensional faults, Plio-Pleistocene volcanic fields (line pattern), springs with mantle ^{3}He (white dots; keyed to Table 2), and Quaternary travertine deposits (keyed to Table 3).

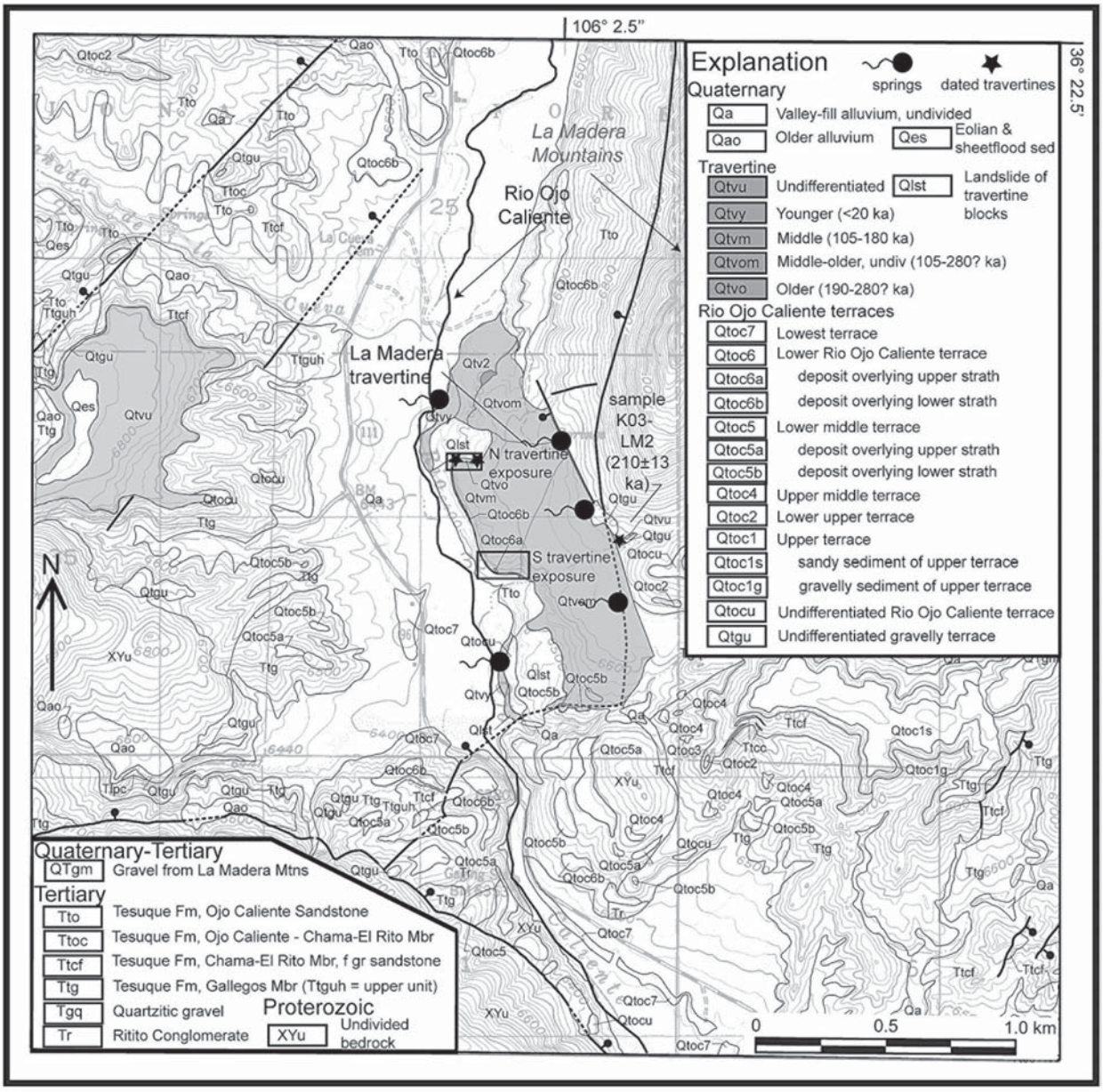

FIGURE 2. Geologic map of the study area (from Koning et al, 2011). Travertines form two prominent platforms: one east of the Rio Ojo Caliente and a higher and older platform on the western side of the valley. Circles indicate the location of the analyzed springs (with two along the river). Locations of the dated travertines are denoted with stars (see Table 3).

are special cases, referring to soil and cave environments of formation specifically. Some workers refer to travertine formed in lacustrine environments as tufa (these are often irregular in shape and highly porous and may contain other minerals than calcite); hot spring deposits, often referred to as sinters, may be composed dominantly of silica. Note that carbon dioxide is a key component of travertine formation. A case of travertine formation in ultramafic rocks in ophiolites and/or serpentinized areas reflects extremely high pH waters that can react with atmospheric or soil gas CO_2 to precipitate travertine. The far more common occurrence (and the mode of formation at La Madera) involves degassing of highly CO_2-charged groundwaters as they emerge at the low- P_{CO2} surface environment, resulting in the precipitation of $CaCO_3$ as travertine.

A groundwater capable of producing travertine necessarily requires both dissolved inorganic carbon (DIC) and calcium. Such a solution is commonly formed when a source of CO_2 combines with water to produce carbonic acid. This corrosive fluid then leaches calcium (among other solutes) from surrounding rock. In some instances (especially geothermal settings), groundwater may leach calcium from silicate rocks. Most importantly, carbonate sedimentary strata are readily soluble by corrosive

fluids and can contribute both calcium and additional carbonate to the dissolved load. The chemical reaction is:

Step 1. $\mathbf{CO_2}_{\text{ (external)}} + H_2O + CaCO_{3\text{ (e.g. limestone)}} \rightarrow Ca^{2+} + 2HCO_3^-$

Step 2. $Ca^{2+} + 2HCO_{3\text{ (in solution)}}^- \rightarrow CO_{2\text{ (degassing)}} + H_2O + CaCO_{3\text{(travertine)}}$

Step 1 represents the acquisition of the solute load from carbonates (e.g. limestone in the aquifer) under some condition of excess CO_2 (shown in **BOLD**) relative to typical atmospheric concentrations. We call this the **external CO_2**. Step 2 represents the degassing of CO_2 and the formation of travertine. Note that the CO_2 that we actually measure at a spring contains the homogenized carbon isotopic composition of both the external CO_2 and any CO_2 from carbonate rocks 'digested' along the hydrologic flow paths. Carbonates encountered along flowpaths are often marine (for example the Pennsylvanian Madera Limestone), with an isotopic $\delta^{13}C$ value that is near 0 permil (‰) relative to the standard (PDB: a marine fossil, the PeeDee belemnite). Importantly, for each mole of carbon precipitated as calcite in travertine, an equivalent mole of carbon dioxide degasses to the atmosphere. Thus extensive travertine accumulations represent only a portion of the CO_2 transported from deep sources to the surface. Also note that large amounts of external CO_2 are required to produce the supersaturated spring waters from which travertine is produced. Large volumes of travertine require a combination of high water discharge, abundant external CO_2, and large amounts of time. The percolation of meteoric water through limestone without a significant external carbon input will not alone provide sufficient chemical 'leverage' to transport the necessary solute load to produce large volumes of travertine. A common example of low external CO_2 systems is the infiltration of meteoric water, with a tenfold increase in CO_2 due to soil microbial respiration - this process results in the formation of many vadose cave speleothems (see Ford and Williams, 2007). Accumulation rates are relatively low (mm/ky), and this external CO_2 is characterized by a low $\delta^{13}C$ value consistent with an organic source on the order of -30 ‰. A high CO_2 system, commonly found in volcanic environments in association with geothermal systems, would be characterized by much higher solute loads, depositional rates as high as cm/yr (though a wide range is observed), and higher $\delta^{13}C$ values of -10 to above 0 ‰ are measured. Examples and case studies may be found in Turi (1986), Fouke et al. (2000), Chafetz and Folk (1984), and Crossey et al. (2006).

Travertine deposition often occurs on slopes (ranging from gentle to steep), with inclined primary bedding. For example, Figure 3 shows both active modern (3a) and extinct older (3b) travertine drapes at La Madera. Laminations and banding are commonly observed at the millimeter- to centimeter scale, and have been shown in many case studies to result from daily and seasonal growth patterns. When degassing is rapid due to turbulence caused by water falls, flow over obstacles, and channel irregularities, the waters become more supersaturated with respect to calcite. Precipitation (formation of travertine rock) takes place, not only at the spring vent (Figs. 4a and 4b), but as hanging curtains associated with waterfalls (Figs. 4c), finely-laminated flowstones,

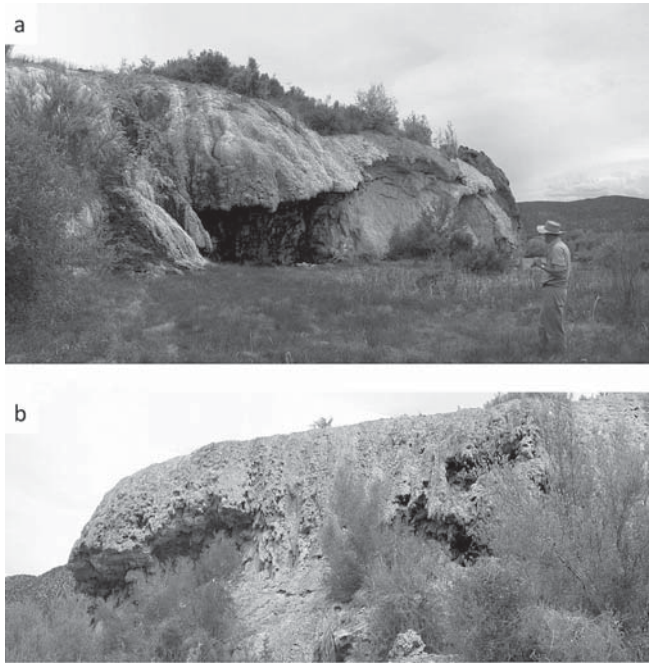

FIGURE 3. a. Holocene travertine drape is forming near river level as CO_2-rich waters pour over and de-gas at vegetated modern waterfall. b. High travertine drape formed in a similar way 100-200 thousand years ago, when river was in a higher landscape position

terraced pools (Figs. 5a and 5b), and coatings on objects in the stream (Fig. 4d). In active systems, a positive feedback between the growth of dam structures and enhanced degassing is very common at scales from millimeters to decimeters. The migration of dam structures on sloping surfaces results in undulatory bedding (Figs. 5a and 5b). Generally, dam spacing decreases as slope steepness increases. Travertines forming in pools behind dams or in marsh environments are rarely bedded and can be micritic suggesting slow calcite precipitation, whereas dams and drapes are typically sparry and fibrous, indicative of higher rates of precipitation. Biological influences may be seen in the form of bacterial and algal laminations; bryophyte, charophyte and reed casts (Fig. 5c); and leaf, stick, and tree casts (Fig. 5d). Distal to spring orifices, carbonate may form as cement associated with alluvium (Fig. 4d). Beautifully banded carbonate cements can form under river water in gravel channels due to groundwater outlets. Caves often develop within drapes and waterfalls due to underflow of water through previously deposited travertine. These deposits can include botryoidal textures indicative of calcite growth into open space (Fig. 5e) and banded flowstone and speleothems (Fig. 5e). Caves within drapes may contain younger calcite as veins and cave infillings within previously deposited travertine while the overall platform is still hydrologically connected and the local groundwater table migrates up or down through the deposit with changing head and flowpaths. These infillings are relatively pure calcite and attractive to date, but they only provide minimum ages on the stratigraphic travertine layers they cross cut (Fig. 6a). Clastic travertine composed of locally-derived intraclasts, as well

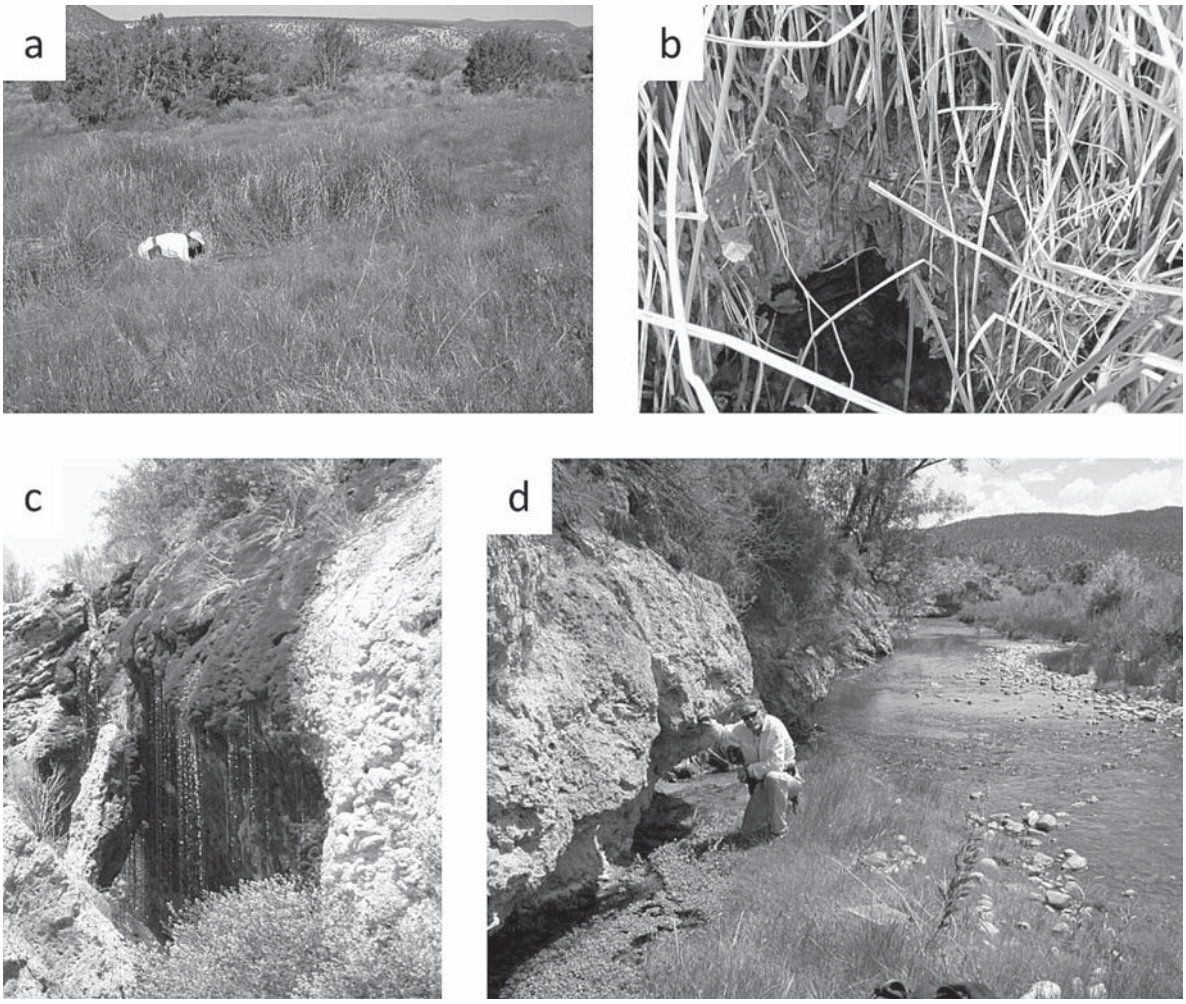

FIGURE 4. Active CO_2-springs in the La Madera travertine area include: a. spring on top of travertine platform, b. spring orifice and ongoing cementation of vegetation, c. waterfall at N end of outcrop is creating the Holocene to ongoing drape. d. underflow through caves pouring out into the Rio Ojo Caliente and cementing modern river gravels.

as slope wash or stream sediments, are also locally abundant. An often overlooked expression of travertine is as calcite cements within fault zones and in regional aquifers.

WATER GEOCHEMISTRY IN THE LA MADERA SPRINGS AND REGIONAL GROUNDWATER IMPLICATIONS

Travertine deposits need to be understood in the context of the waters that deposit them. Travertine-depositing spring waters are distinctive—they commonly represent the mixing of "upper world" (epigenic) groundwaters derived from surface recharge with "lower world" (endogenic) fluids that carry very high mineral loads (dissolved salts) and high levels of carbon dioxide and other exotic gases from deep within the Earth. While the springs can issue from specific stratigraphic horizons, at La Madera and many other locations in northern New Mexico they are also associated with faults. The active travertine-depositing springs provide a window into subsurface hydrologic mixing of shallow and deep fluids.

The traditional view of the hydrologic cycle focuses on connections to Earth's surface-water circulation. Surface water, derived from snow melt and rainfall percolate through near-surface sediments and rocks over thousands of years to become deep groundwater. But, while important, the top-down water story is incomplete. A more complete model (Crossey et al., 2006; 2009) considers an additional "lower world" component to the groundwater system: deeply circulated groundwaters that rise along fault conduits and mingle in the groundwater system, occasionally, as at La Madera, emerging through spring vents. The relative proportion of the upper world and lower world waters differs from spring to spring and can be determined by analyzing the water chemistry and especially certain distinctive tracers, or chemical travelers, from the deep. The travertine-depositing springs are a subset of groundwaters with very special characteristics. For example, their flow is relatively constant, they are commonly

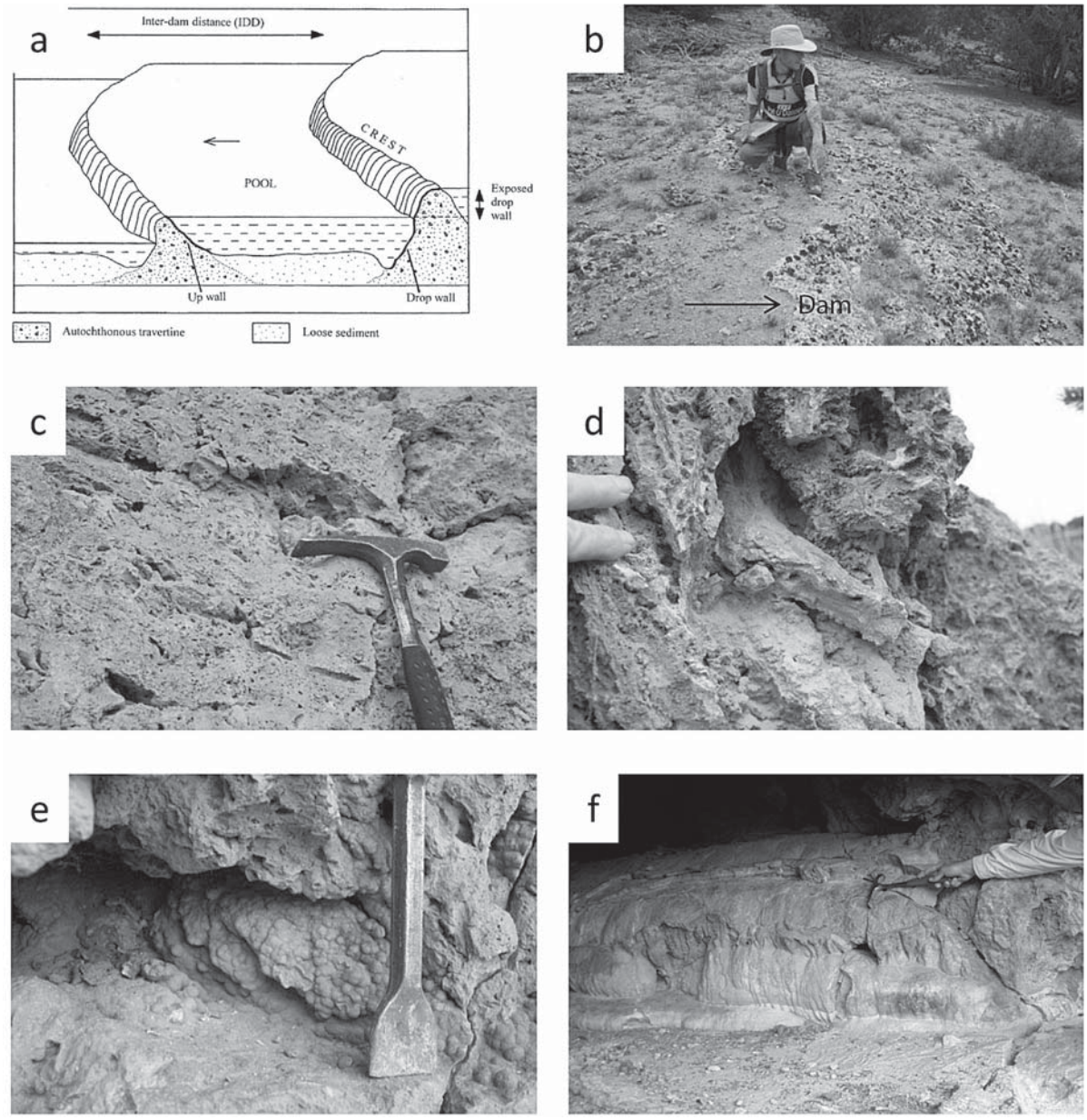

FIGURE 5. Travertine facies: a. Schematic of travertine rimstone dams (modified from Pentecost, 2005); b. observed sinuous rimstone dams on top of La Madera travertine platform; c. porous facies represents cementing of vegetation. d. large stick casts in travertine, e. botryoidal textures, f. flowstone textures in caves indicates underflow through drapes; sample K03-LM5, from location of chisel, is 89 ka (see Table 2).

warm, and low in dissolved oxygen. Thus, sidestreams containing base flow derived from such springs do not provide habitat suitable for fish species such as trout, which require colder, oxygen-rich waters. However, the travertine springs do provide habitat for many endemic species (especially invertebrates and other aquatic life) and the mouths of these sidestreams are preferred breeding areas for fish such as the endangered humpback chub (along the Colorado River) and the desert pupfish in the American Southwest. The geochemistry of these waters and the gases they contain tell a remarkable tale about the origin of the waters and the resulting travertine deposits (Crossey et al., 2006; 2009).

Table 1 presents water chemistry for springs, groundwaters, and the Rio Ojo Caliente in the La Madera area. Geochemical modeling (using PHREEQC, Parkhurst, 1995) shows that, especially near spring sources, the waters show extremely high partial pressures of CO_2. Spring sources are typically undersaturated with calcite at these high PCO_2 values, but would be highly supersaturated as degassing of CO_2 occurs (note that calcite saturation indices tend to increase as PCO_2 of waters decreases in Table 1). Figure 7 is a Piper diagram that shows the geochemistry of La Madera spring waters compared to other groundwaters in the region. In this diagram, cations are plotted in the lower left

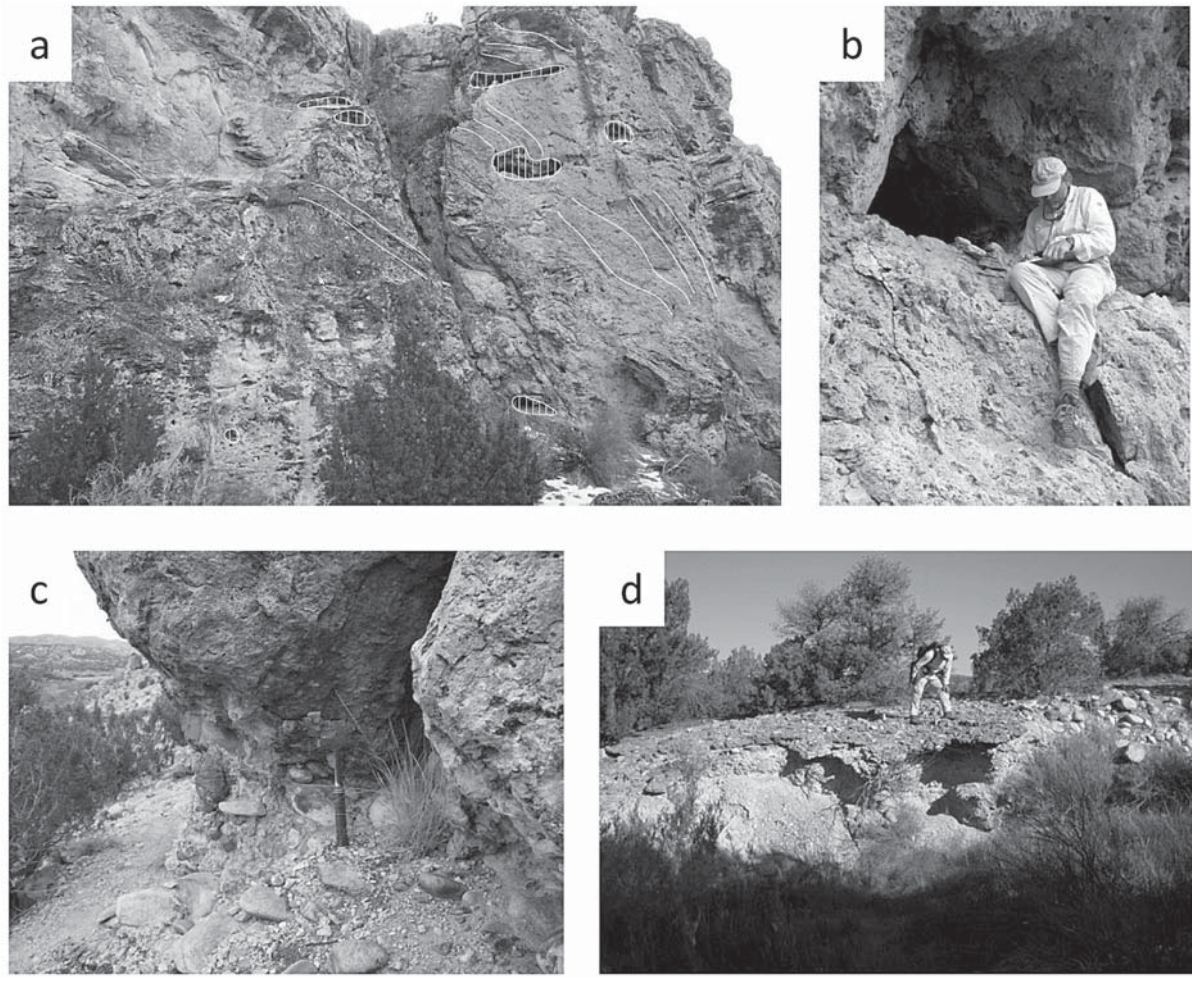

FIGURE 6. a) North travertine exposure of Fig. 2, showing drape and caves (thin white lines and closely-spaced vertical lines, respectively). The 103 ± 0.5 ka age is from a cave below and right of this photo, so the travertine depicted is interpreted to predate 103 ka. Figure 6b) Cave from which Sample K03-LM5 was obtained (89 ± 2.25 ka). This cave is to the left of Fig. 6a. Figure 6c) travertine-cemented gravels of the 20-40 m terrace are overlain by the >103 ka travertine drape. Figure 6d) Dating of travertine-cemented gravels within different river terraces is underway and will provide better constraints for incision rate changes through time.

ternary triangle, anions in the lower right triangle, and both are projected into the central parallelogram. Different areas group nicely into hydrochemical facies. Hydrothermal waters of the Valles caldera and other hot springs plot near the right apex of the parallelogram, in a field that has high Cl, Na, K, and TDS. These waters are interpreted (Crossey et al., 2009) to be close to the "lower world" endmember for mixing of fluids in the aquifer. Low TDS springs and meteoric recharge plot near the left apex of the parallelogram and these are interpreted to be the upper world endmember. Note that water volumes are dominated by this meteoric endmember, but water chemistry can be dominated by relatively small volumes of the lower world endmember. The Rio Ojo Caliente (sampled near base flow) increases in total salinity (TDS; see Table 1) by 46% due to spring inputs along the La Madera travertine reach. La Madera spring waters fall in an intermediate position on Figure 7 suggesting mixing of these endmembers. Other spring groups also cluster based on their distinctive geochemistry and hence suggest different mixing proportions. When considered regionally, the spring groups seem to make a near continuum of endmember mixing.

Similar chemical mixing trends to La Madera are observed within dozens of spring waters analyzed throughout the New Mexico region (Newell et al., 2005; Crossey et al., 2009; Williams, 2009; Jochems et al., 2011). Even dilute springs and the Buckman groundwater well fields that are used for water supply for the city of Santa Fe reflect variable lower world inputs that degrade water quality. The Chimayo CO_2 geyser, and spring waters near San Ysidro also show mixing of lower and upper world sources. Important trace elements in these spring waters include arsenic, silica, uranium, lithium, fluorine, boron, bromine, and barium. These elements reflect fluid circulation, mixing with hydrothermal inputs, and rock-water interaction with volcaniclastics (that

TABLE 1. La Madera Spring Chemistry

Sample ID	Name	Spring Location Dec. Lat Long (NAD 83)	T (C)	pH	[1]TDS ppm	Ca ppm	Mg ppm	Na ppm	K ppm	Alkalinity ppm	Cl ppm	SO4 ppm	[2]Charge balance %	[3]log PCO2	[4]S.I. calcite
AK-LM-09-63	La Madera Spring Group	36.3608, 106.0421	26.2	5.87	1388	125	53	165	14	647	106	278	-3.3	-0.1	-0.85
AK-LM-09-64	La Madera Spring Group	36.3609, 106.0425	14.2	7	1539	110	63	191	16	683	137	339	-6.6	-1.3	0.06
AK-LM-09-65	La Madera Spring Group	36.3524, 106.0430	12.9	7.04	1341	93	52	171	14	653	107	252	-6.3	-1.3	0.02
AK-LM-09-66	La Madera Spring Group	36.3524, 106.0430	13.2	6.95	1325	95	52	167	14	628	116	253	-6.2	-1.3	-0.07
BE-03-OJO-1	La Madera Spring Group	36.3565, 106.0416	22.9	8.13	1649	62	73	298	23	765	146	283	0.2	-2.3	1.08
LC-03-LM-10	Rio Ojo Caliente at Bridge	36.3511, 106.0453	15.3	8.11	830	85	34	95	9	444	53	110	1.5	-2.6	0.97
LC-03-LM-11	La Madera Spring Group	36.3511, 106.0453	14.2	7.76	1638	95	77	234	20	785	195	231	-3.2	-2.0	0.82
LC-03-LM-12	La Madera Spring Group	36.3605, 106.0421	25.9	6.03	1374	137	63	175	16	670	94	220	4.6	-0.2	-0.63
LC-03-LM-13	Rio Ojo Caliente at Waterfall	36.3641, 106.0473	23.3	8.06	567	65	17	55	5	335	31	59	-2.9	-2.6	0.85
LC-03-LM-14	La Madera Spring Group	36.3605, 106.0421	22.1	6.63	1220	110	64	78	16	633	96	224	-9.8	-0.9	-0.19
LC-03-LM-15	La Madera Spring Group	36.3605, 106.0421	16.4	6.51	1220	129	43	178	11	584	82	194	6.0	-0.8	-0.35
LC-03-LM-16	Statue Spring	36.3819, 106.0605	28.2	6.05	1275	110	59	166	15	634	87	204	2.4	-0.3	-0.69
LC-03-LM-20	La Madera Spring Group	36.3565, 106.0416	18.3	6.17	1443	130	62	182	16	778	89	186	2.0	-0.4	-0.55
LC-03-LM-22	La Madera Spring Group	36.3609, 106.0425	25.9	6.15	1360	137	63	175	15	656	93	221	5.3	-0.4	-0.52
LC-03-LM-25	Atterbury Well	36.3537, 106.0491	17.1	7.04	1674	64	12	438	7	920	71	162	6.7	-1.2	0.07
LC-09-CH3	Chimayo Well	35.9922, 105.9445	14.1	6.12	7092	424	186	1022	48	3978	1122	312	-11.5	0.3	0.30

[1] TDS is total dissolved solids, computed as the sum of major ions expressed in parts per million (ppm).

[2] Charge balance computed as the sum of cations minus the sum of anions normalized to the combined sum (all in meq/L).

[3] Partial pressure of CO_2 with which the water has equilibrated using the geochemical modeling code PHREEQC (Parkhurst, 1995).

[4] degree of supersaturation (Saturation Index) with respect to calcite computed using PHREEQC.

can be high in As), granites (that are high in U and Radon), and mineral deposits (e.g. roll-front deposits in the Española Valley; McLemore et al., 2011). In most cases, the presence of these dissolved constituents impairs the water quality, making the waters less fit for human consumption.

In summary, our hypothesis is that mixing of chemically potent, deeply sourced, endogenic fluids degrades groundwater quality in direct proportion to the mixing percentages of epigenic and endogenic inputs. Epigenic waters are characterized by low salinity, Ca-Mg-bicarbonate fresh water compositions typical of meteoric recharge and limestone aquifers. Endogenic water components have high CO_2, lower pH, high salinity, and high alkalinity, with variable trace and major element compositions typical of hydrothermal waters (Table 1). This model provides an avenue for mitigation of water quality degradation via management procedures that involve deliberate mixing of variable groundwater and surface water sources.

GAS COMPOSITION, ^{3}HE/^{4}HE DATA, AND EVIDENCE FOR MANTLE CONTRIBUTIONS IN SPRINGS

In addition to CO_2, an isotope of helium (^{3}He) is found in quantities higher than expected in groundwater in all of these springs. Much of the Earth's ^{3}He is primordial, left from Earth formation, and this isotope is relatively abundant in the mantle (Clarke et al., 1969). ^{3}He can also form in small quantities in the near-surface system from lithium spallation, cosmic rays, and beta decay of tritium. But, when ^{3}He is found in large abundances in non-air-contaminated waters at spring vents (where we sample), it is the "silver bullet" tracer for identifying volatiles from the mantle. This indicates that the same sort of tectonic processes necessary to produce volumes of basalt (also prevalent in the rift) is yielding the CO_2-rich fluids that rise along faults and mingle with groundwaters coursing through the regional fault systems and leaking into local aquifers. The presence of mantle-derived helium provides unequivocal documentation of a remarkable connection between the mantle, movement of small volumes of lower world fluid up along faults, and mixing with the much higher volume water in the aquifer, to produce quite variable chemistry of springs and groundwaters.

In contrast, the isotope ^{4}He accumulates from radioactive decay of U- and Th-series nuclides, which tend to be concentrated in the crust. We measure the ^{3}He/^{4}He ratio of spring waters collected right at the vent to avoid air contamination. This ratio is typically reported (normalized) relative to air ($R_A = 1.4 \times 10^{-6}$). For context, mantle-derived fluids at mid-ocean ridges, derived from the upper mantle, have values of 8 ± 1 R_A (Graham, 2002), whereas hot springs at Yellowstone Park, derived from a plume tapping deeper, less degassed portions of the mantle, have ^{3}He/^{4}He values of ~16 R_A (Craig et al., 1978). Continental cratonic areas have values of 0.02 R_A consistent with extensive addition of ^{4}He from radioactive decay (Reid and Graham, 1996) in areas that have been shielded from any recent asthenospheric inputs by thick lithosphere. Values greater than 0.1 R_A are typically taken as strong evidence for a young (last several million year) input of mantle-derived volatiles. Regional studies (Newell et al., 2005) indicate that most of the CO_2-rich springs of the western U.S. springs contain measurable mantle components, with the highest values concentrated along plate margin fault systems and near volcanoes. There is also an association of high mantle helium with low seismic velocity mantle domains which is interpreted to reflect regional and widespread mantle degassing throughout the tectonically active western U.S., and as far east as the western Great Plains (Newell et al., 2005).

Figure 1 shows the distribution of hot and cool springs in northern New Mexico that have been analyzed for their helium isotope composition; and Table 2 summarizes ^{3}He/^{4}He isotopic data from northern New Mexico. Air corrected ^{3}He/^{4}He values

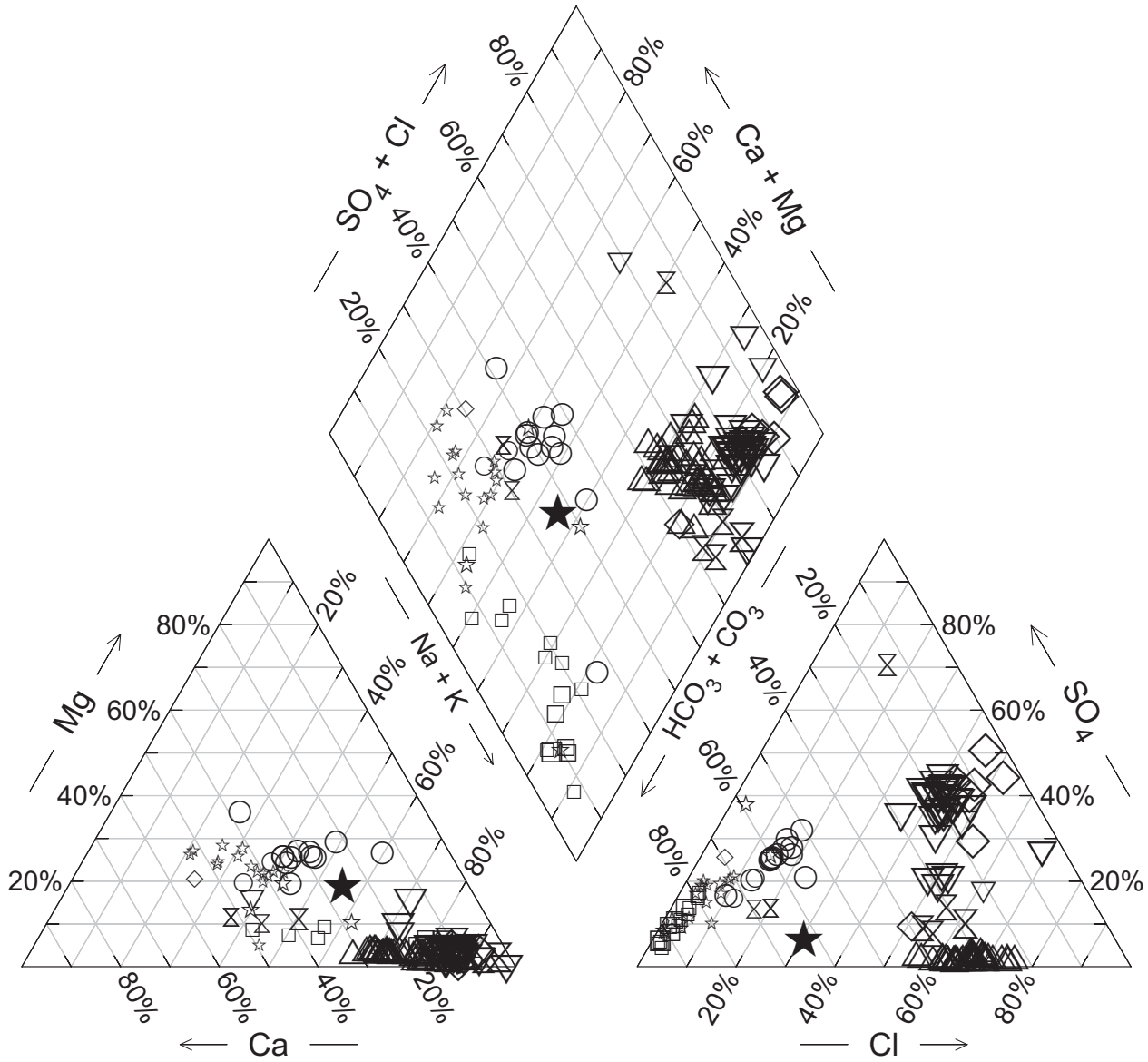

FIGURE 7. Piper diagram (Piper, 1944) of water chemistries in northern New Mexico. Symbol size varies according to salinity: see Table 1. Buckmen Well field (squares), Chimayo Geyser (large filled star), Jemez Pueblo (diamonds), La Madera (circles), Rio Grande springs (stars), Tierra Amarilla near San Ysidro (down triangles), Valles Caldera (up triangles), Zia Pueblo (hourglass). Buckman well data from Johnson et al., 2008; Jemez Pueblo data from Craigg, 1984; other data from Newell et al., 2005.

range from 0.1 to 6.1 R_A. The highest $^3He/^4He$ values are in the Valles caldera, where waters and gases from both surface springs (Sulfur Springs; up to 5.16-6.16 R_A) and hydrothermal test drill holes (VC wells; 5-5.72 R_A) indicate 60-77% of the He is from the mantle. $^3He/^4He$ values decrease rapidly both SW and NE of the Caldera, but values of 0.33 R_A at both La Madera and San Ysidro attest to appreciable (4%) mantle helium at considerable distance from the caldera. Our interpretation of this pattern is that, like much of the western U.S., mantle degassing from faults is regional. The very high values in the caldera reflect the presence of a shallow magma body present there (Lutter et al., 1995; Roberts et al., 1995; Goff, 2009) and suggest that hydrothermal pressure gradients may drive fluid circulation along faults to the SW (the Baca plume of Goff and Gardner, 1994) and perhaps also to the NE of the caldera.

MODELING OF SOURCES OF CO_2

There are several possible sources of the CO_2 gas that acts as the carrier gas for the mantle-derived helium and is also the key agent that makes the water corrosive enough to dissolve limestone in the flow path. For the past few decades, most workers

TABLE 2. Helium and carbon isotopic data from CO_2-rich springs in northern New Mexico

Map #	Location name	T (°C)	R_C/R_A [a]	$CO_2/^3He$ (x 10^9)	% Mantle He [b]	$\delta^{13}C$ (‰) [c]	Reference
1	Chimayo geyser well	15	0.65	nd	8.1	-5.93	Goff and Janek (2002)
	Chimayo geyser well	15	0.518	140988	6.5	-20.5	this study
2	Jemez Pueblo- Salt Spring	14.5	0.114	133	1.4	nd	Newell et al. (2005)
	Jemez Pueblo- Upper Owl Spring	15.5	0.384	nd	4.8	nd	Newell et al. (2005)
	Jemez Springs n=2	75	1.27	nd	15.9	-5.15	Goff and Janek (2002)
3	Jemez River- Soda Dam n=3	47	0.84	418	10.5	-4.9	Goff and Janek (2002)
4	John Dunn Bridge (Black Rock) hot springs	36	0.09	nd	1.1	nd	Newell et al. (2005)
5	La Madera Travertine	26.2	0.33	456	4.1	-2.2	Newell et al. (2005)
6	Manby (Stagecoach) Hot Spring- bathhouse	37	0.316	nd	4.0	nd	Newell et al. (2005)
	Manby Hot Spring- S of bathhouse	37.9	0.301	nd	3.8	nd	Newell et al. (2005)
7	Ponce De Leon warm spring	32.7	0.199	nd	2.5	nd	Newell et al. (2005)
8	Tierra Amarilla anticline- twin mounds (LC07SY1)	25	0.17	79.4	2.1	-8.71	this study
	Tierra Amarilla - Grassy Spring	24.5	0.198	42	2.5	-4.6	Newell et al. (2005)
9	Valles caldera- Baca Wells n=10	270	4.75	3.91	59.4	-4.95	Goff and Janek (2002)
	Valles caldera- Sulfer Spring- footbath spring n=12	20	5.16	1.13	64.5	-2.47	Goff and Janek (2002)
	Valles caldera- Sulfer Spring- womens bathhouse n=4	88	6.16	2.86	77.0	-3.6	Goff and Janek (2002)
	Valles caldera- VC-2A well n=7	210	5	6.94	62.5	-4.95	Goff and Janek (2002)
	Valles caldera- VC-2B well n=3	295	5.72	2.37	71.5	-3.3	Goff and Janek (2002)
10	Zia hot well	54	0.23	nd	2.9	-6.77	Goff and Janek (2002)
	Zia C-spring	19	0.32	nd	4.0	-5.25	Goff and Janek (2002)

nd = not determined

[a] R_C/R_A = air saturated water corrected R/R_A using $(R_C/R_A) = ((R/R_A)X-1)/(X-1)$ where X is the air-normalized (He/Ne) ratio multiplied by the $ß_{Ne}/ß_{He}$ at 15°C (Ozima and Podosek, 1983) where $ß_{Ne}$ and $ß_{He}$ are the Bunsen solubility coefficients for neon and helium in pure water; $R_A = {}^3He/{}^4He$ in air= 1.4 E-06

[b] percent mantle He of the total He in sample= $[(R_C/R_A)/8$ (MORB-source value)] x 100

[c] $\delta^{13}C$ was measured from dissolved DIC in water for most springs: Valles hydrothermal samples are reported as $\delta^{13}C$ from exsolved gases; $\delta^{13}C$ reported in permil (‰) versus PDB. The one-sigma error on $\delta^{13}C$ is ±0.2 ‰

have thought that the elevated CO_2 necessary to make the groundwaters corrosive was acquired in the recharge areas, through near-surface biological respiration and other microbial activity in soils and due to transpiration of plants (Giegengack and Gaines, 1979; Chafetz and Folk, 1984; Monroe et al., 2005).

However, our recent work in the tectonically active western U.S. demonstrates that this is not the case, and that the primary origin for much of the CO_2 is found deep in the Earth and is tectonic in origin. When we actually trap and analyze the gases emanating from the springs, we find that the bubbles coming out of solution are, other than water vapor, nearly pure CO_2. The source of this CO_2 is found by measuring its isotopic composition and examining other trace gases in the springs (described in Crossey et al., 2006; 2009; Newell et al., 2005, 2008).

The extent to which New Mexico hot and cool springs are CO_2-rich is manifested by the travertine deposits around springs, and by the P_{CO2} values that are several orders of magnitude above atmospheric (Table 1). Water chemistry can be used to model sources of CO_2 following methods outlined in Crossey et al. (2009) and Chiodini et al. (2004). Sources contributing to the CO_2 load of springs include: 1) dissolution of carbonates along flow paths (C_{carb}), 2) carbon of organic origin (C_{org}), including biologically respired CO_2 and soil gas, and 3) inputs of endogenic CO_2 stored and/or generated in the crust and mantle (C_{endo}). Water chemistry can be used to estimate the proportion of CO_2 derived from dissolution of carbonate. In Colorado Plateau and most New Mexico waters, this value is less than 20-50% (Crossey et al., 2009). After the C_{carb} is accounted for, the measured $\delta^{13}C$ of each spring can be used to estimate the proportions of soil- respired CO_2 endmember ($\delta^{13}C_{org}$ = -28 ‰; Deines, 1974) and endogenic CO_2 endmember ($\delta^{13}C_{endo}$ = -3 to -5‰). Most springs in northern New Mexico have $\delta^{13}C$ of -2 to -8 per mil (Table 2) suggesting a high proportion of endogenic CO_2 relative to organic-derived CO_2 in the groundwaters. We interpret this high endogenic CO_2 of New Mexico springs to reflect the tectonically active geologic setting where many springs emanate from faults and carry mantle-derived CO_2. The Chimayo geyser well has values that range from -6 to -20‰, interpreted to reflect stripping of and fractionation of CO_2 gas during gas-groundwater interaction and near surface degassing (e.g. Gilfilan et al., 2008, Newell et al., 2008).

$CO_2/^3He$ ratios can also be used to evaluate sources of CO_2. Mid Ocean Ridge Basalt (MORB) $CO_2/^3He$ is about 2 x 10^9 (7.5

x 10^8 - 3 x 10^9 , Sano and Marty, 1995), whereas this ratio in continental areas is up to 5 orders of magnitude higher (O'Nions and Oxburgh, 1988). Springs of New Mexico have $CO_2/^3He$ ratios that range from 1-2 x 10^9, to 10^{15}. Hydrothermal areas of the Valles caldera have values of 1-6 x 10^9, which is consistent with a dominantly mantle source for the CO_2. At the other extreme, Chimayo geyser has a value of 10^{15}, interpreted to reflect CO_2 gas fractionation and stripping from groundwater. $CO_2/^3He$ values of 10^{11} in many springs (e.g. 4.56 x 10^{11} at La Madera) suggest mixing of mantle values with CO_2 stored in the subcrustal lithospheric mantle and crust (Crossey et al., 2009) and fractionation of CO_2 in the shallow groundwater system (Ray et al. 2009; Gilfillan et al., 2008).

TRAVERTINE AGES AND IMPLICATIONS FOR PALEOHYDROLOGY AND PALEOCLIMATE

Advances in geochronology using uranium-series dating, combined with geochemical and geologic studies, makes travertine very useful for better understanding of landscape evolution (for example the incision of the Rio Ojo Caliente; Koning et al., 2011) and of climatic variability. Pioneering work on dating Grand Canyon travertine deposits was done by Barney Szabo of the U.S. Geological Survey (Szabo, 1990) and we are expanding this work with recent very detailed studies of geologically well-constrained units throughout the Colorado Plateau and Rio Grande rift. The new dates have implications for reconstructing climate (e.g., Pentecost, 1995), timing of local hydrologic changes, and river incision (Pederson and Karlstrom, 2001; Pederson et al., 2002, 2006; Karlstrom et al., 2007, 2008). Carbonates in subsurface cave deposits (speleothems and other karst formations) are the subsurface cousins to travertine deposits and these have also been used to produce excellent paleoclimate and paleohydrology records in the region (e.g., Winograd et al., 1992; Asmerom et al., 2010). Paleoclimate studies utilizing travertine are just beginning and offer rich potential to provide datable continental records of changes in the landscape and hydrologic system through time. In particular, these deposits have potential to test evolving concepts of how desert environments reacted to global glacial/interglacial climate cycles. Past positions of the walls of drainages and hillslopes can be seen where armoring by travertine has provided a resistant cover in areas where stream valleys have progressively widened and where, in wetter past hydrologic conditions, springs gushed from vents that are now dry. Thus, travertines form a rare link between the paleoclimate record, a record of landscape change, and the modern groundwater system.

Table 3 provides a summary of U-series dated travertines of northern New Mexico. Of interest in the tabulation of Table 3, the Soda Dam and Tierra Amarilla (San Ysidro) deposits are beginning to yield a record of the transition from the penultimate glacial maximum (135 ka), the midpoint of the transition (~130 ka), and the ensuing interglacial (125 ka) that is documented globally by the transition from oxygen isotope stage 6 to oxygen isotope stage 5 (Shackleton et al., 2003).

The relationship of deposition of large travertine volumes to paleohydrology and paleoclimate is still under investigation and requires multiple working hypotheses, applied area to area. 1) If flux of external CO_2 is steadily and voluminous enough to supersaturate local groundwater supply, then deposition of large volumes of travertine may be "water controlled" in the sense that more groundwater discharge would produce more travertine during cooler and wetter paleoclimates (glacials) and, conversely, travertine deposition would be limited during dryer periods (interglacials). However, 2) if large groundwater fluxes can overwhelm available external CO_2 and dilute springs, large volume travertine deposition might be "CO_2- limited" such that large volumes of travertine might be expected during warmer/ dryer paleoclimates (interglacials). 3) A tectonic version of the "CO_2-limited" model might envision that CO_2 flux is episodic due to seismicity and volcanism and hence large volumes of travertine deposition may be related primarily to tectonics and should show no systematic correlation with paleoclimate and paleohydrology shifts.

Figure 8 shows available travertine dates from northern New Mexico plotted on a timeline that also shows global glacial periods (shaded and even numbers) and interglacial periods (white and odd numbers) based on the marine oxygen isotope stage (MIS) record (Karner et al., 2002). Also shown are regional climate proxies from New Mexico (Fawcett et al., 2011; Asmerom et al., 2010), and a southeastern California record (Winograd et al.; 1997). Existing data show that travertines have been deposited during both glacial and interglacial paleoclimates. Our current effort is to estimate when the largest volumes were deposited (Priewisch et al., 2011). We are also beginning to date and use climate proxies for continuous records preserved in calcite feeder veins that are found in the cores of some travertine mounds and that record key climate transitions (Tafoya et al., 2011). Soda Dam offers a good record across the sharp transition (deglaciation) from glacial times of MIS 6 to the complex interglacial conditions of MIS 5. Both Soda Dam area and Tierra Amarilla (San Ysidro area) contain a record of MIS 5.

Timing constraints for the MIS 6 to 5 climatic transition (Shackleton et al., 2003) suggest rapid deglaciation in a timespan as short as 4-10 ka, and a New Mexico record of this important timeframe will be examined at Soda Dam. Key global datapoints as summarized by Shackleton et al. (2003) include: 1) the marine low stand and inferred glacial maximum perhaps as late as 132 ± 2 ka (Esat et al., 1999), or 2) the midpoint of the Stage 6-5 transition at 135 ± 2 ka (Henderson and Slowey, 2000), 3) the MIS 5e highstand and interglacial "plateau" at 129 ± 1 (Cutler et al., 1999) to 128 ± 1 ka (Stirling et al., 1998), 4) the start of the marine regression that marks the termination of MIS 5e at 116.1 ± 0.9 ka; Shackelton et al., 2003), and 5) MIS 5a marine highstand at 82.9 ± 0.4 ka (Edwards et al., 1997).

LINKS TO NEOTECTONICS AND LANDSCAPE EVOLUTION

Figure 1 shows the locations of travertine occurrences in northern New Mexico and Table 3 summarizes existing age constraints based on U-series dating. Extensive travertine mounds and platforms developed due to persistent degassing along the NE-trending faults associated with the Jemez lineament, Valles caldera,

TABLE 3. Locations and U-Series ages of travertines in northern New Mexico

Map #	Location Name	Age (ka)	error +	error -	Elev. above base level (m)	Description of Travertine	MIS Stage	Interpetation of U-Series ages	Reference
2	**Jemez Pueblo**								
	Blue Water Spring area					along N-S Jemez fault and NE trending San Ysidro fault			Woodward and Ruetschilling, 1976
3	**Jemez River Soda Dam**								
	Soda Dam	4.80	0.02	0.02		base of NW-trending fracture	1	Soda Dam began growing at 4.8 ka	Goff and Shevenall, 1987
	Deposit B	58.00	3.00	3.00		spar travertine near core of mound	3		Goff and Shevenall, 1987
	Deposit B	78.20	1.60	1.60		top of deposit B	5	end of wet period	Tafoya et al., 2011
	Deposit B	98.00	7.00	7.00		travertine near summit of mound	5	end of activity in this mound	Goff and Shevenall, 1987
	Deposit B	138.40	1.10	1.10		near base of travertine mound	6	near end of MIS stage 6- beginning of wet period	Tafoya et al., 2011
	Deposit C	101.70	0.50	0.50		top of deposit C	5	end of deposition in this deposit	Tafoya et al., 2011
	Deposit C	103.20	0.50	0.50	16.5	travertine immediately overlying strath	5	incision rate of 160 m/Ma over last 100 ka	Tafoya et al., 2011
	Deposit C	107.00	5.00	5.00		sill of spar travertine travertine near base	5	same depositional event as deposit B	Goff and Shevenall, 1987
	Deposit A	183.10	2.10	2.10	33	travertine drape above base of accumulation	6	springs were poring into the river	Tafoya et al., 2011
	Deposit A	200.60	2.10	2.10	30	calcite rinds on river gravels at N end of cave area	7	incision rate of 150 m/Ma over last 200 ka	Tafoya et al., 2011
	Deposit A	215.00	40.00	40.00	2121	spar sill that cross cuts micritic layering	7	recrystallized, low 234/238; age may be incorrect	Goff and Shevenall, 1987
	Deposit A	> 350 ka				higher travertines of deposit A		outside U-Series range: considered >350 but < 1 Ma	Goff and Shevenall, 1987
4	**La Madera Travertine**								
	K03-LM5	89.24	2.22	2.18		flowstone in cave	5	later depostion in high travertine platform?	this paper
	K03-LM4	103.16	3.15	3.08		flowstone in cave that crosscuts drape, elev	5	minimum age on 20-40 m gravel terrace	this paper
	K03-LM2	210.50	13.57	12.37		layered calcite vein cuts cemented sidestream terrace	7	minimum age of Qt 6 of Newell et al. (2005)	this paper
7	**Tierra Amarilla anticline area N side of highway**								
		30.60	0.30	0.30	36	travertine cementing elevated terrace gravels	3	age of Qt4 gives 116 m/Ma incision rate	Rose-Coss et al., 2008
		250.00			63	travertine cementing elevated terrace gravels	8	age of Qt6 gives 252 m/Ma incision rate	Rose-Coss et al., 2008
		415.00	0.20	0.20	140	travertine cementing elevated terrace gravels	11	age of Qt8 gives 337 m/Ma incision rate	Rose-Coss et al., 2008
9	**Zia Penasco Canyon**								
		57.50	0.50	0.50	13-35	travertine overlies Qt2 terrace and fault	3	overlies Qt2, incision of 217 m/Ma since 60 ka.	Formento- Trigilio and Pazzaglia, 1998
		63.50	0.60	0.60	13-35	travertine overlies Qt2 terrace and fault	4	overlies Qt2, fault slip of 13 m/Ma	Formento- Trigilio and Pazzaglia, 1998
		272.00	24.00	24.00	13-35	cements Qt2 gravels is offset by 4.2 m	8	age of Qt2 , bedrock incision rate of > 477 m/Ma	Formento- Trigilio and Pazzaglia, 1998

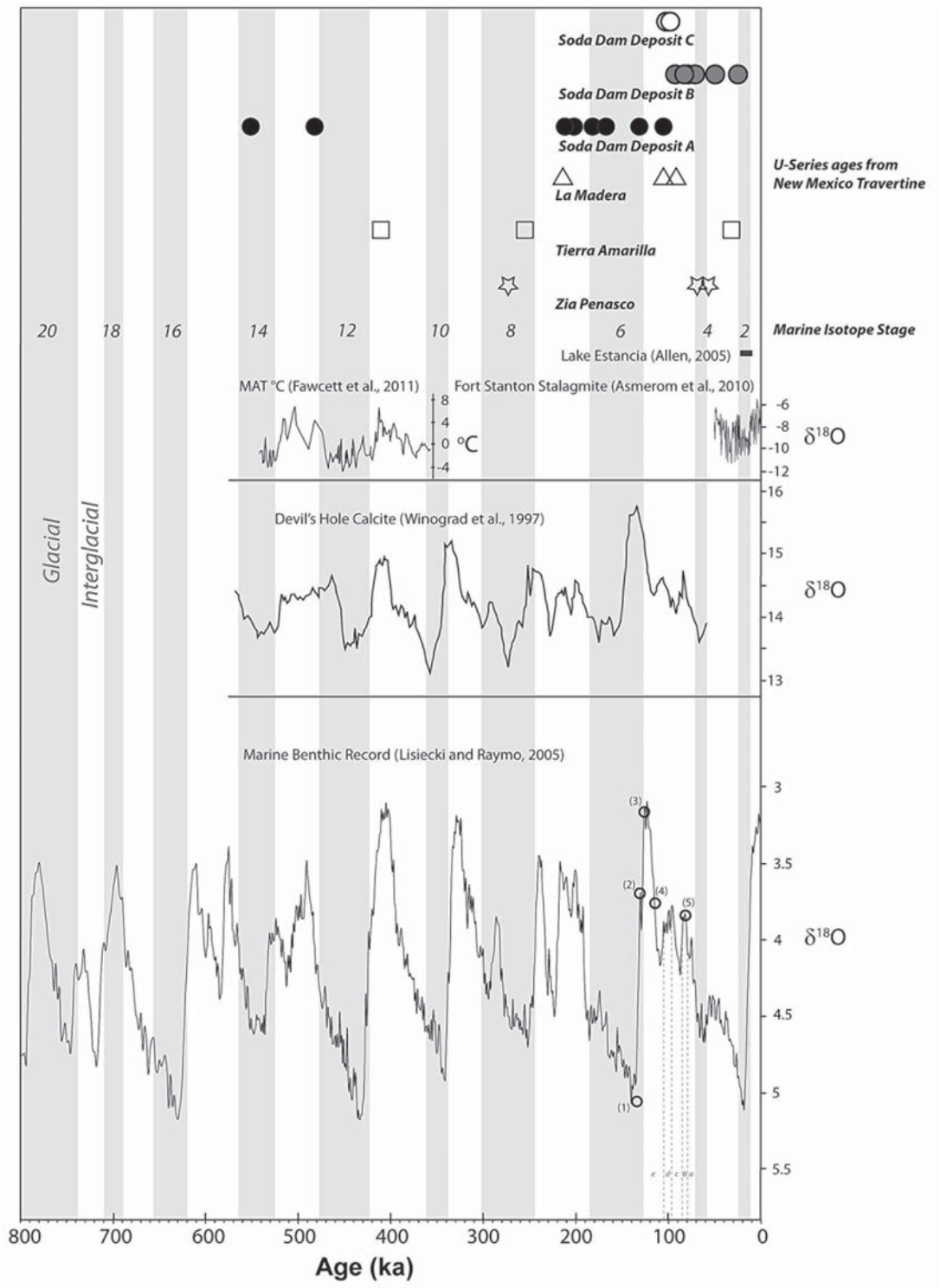

FIGURE 8. Timeline of travertine deposition from locations in northern New Mexico in the context of paleoclimate records. Travertine ages, obtained by U-series geochronology, are shown at top from different areas. Error bars are smaller than plotted symbols for most samples. Global glacial periods (shaded and even numbers) and interglacial periods (white and odd numbers) are shown by marine isotope stages (MIS) from Lisiecki and Raymo (2005). Regional climate proxies are from Fawcett et al. (2011); Asmerom et al. (2010) and Winograd et al. (1997). Duration of Lake Estancia from Allen (2005). Key dates for the MIS 6 to 5 transition are from Shackelton et al. (2003): 1) Midpoint of the Stage 6-5 transition (135 ± 2 ka; Henderson and Slowey, 2000), 2) 60 – 80 m lowstand documented in Aladdin's Cave at 132 ± 2 ka from Esat et al. (1999) 3) MIS 5e highstand (128 ± 1 ka; Stirling et al., 1998), 4) Start of marine regression (116.1 ± 0.9 ka; Shackelton et al., 2003), 5) MIS 5a maxima (82.9 ± 0.4 ka; Edwards et al., 1997).

and the Embudo transfer zone of the Rio Grande rift. Voluminous deposits occur both in the Jemez River and San Ysidro areas, and NE of the Jemez Mountains at La Madera.

Existing U-series ages show that travertines record a > 500 ka history of deposition. Travertines provide some of the most precise dates for calculating bedrock incision rates (Table 3). The incision significance of the dated travertines at La Madera is discussed in Koning et al. (2011a; see also Newell et al., 2004). Additional dating is underway to refine the chronology of both the La Madera cliff section and the high travertines across the valley and along the road to El Rito. Parallel dating efforts are underway in the Jemez River (San Diego Canyon near Soda Dam) giving rates of 150 m/Ma over the last 200 ka (Tafoya et al., 2011). Travertines of the Rio Salado area west of San Ysidro give variable and generally declining incision rates but a long term rate of 337 m/Ma over the last 415 ka, which is one of the highest bedrock incision rates in New Mexico (Sower et al., 2008; Rose-Coss, 2008). Travertines along the Nacimiento fault also give high incision rates of > 200 m/Ma (Formento- Tigilio and Pazzaglia, 1998).

CONCLUSIONS

This paper describes features of the La Madera spring and travertine deposits that are similar to other regional occurrences in northern New Mexico. Several of these features are interpreted as evidence for a linked neotectonic system along the Jemez lineament near its intersection with the Rio Grande rift. These neotectonic signals are: 1) CO_2- rich springs along faults, 2) voluminous travertine accumulations indicative of dominantly external (deeply derived) CO_2, 3) elevated $^3He/^4He$ composition indicative of a mantle origin for part of the fluid, and 4) high and spatially variable incision rates derived from travertine U-series dating of river terraces. All are interpreted to reflect dynamic uplift of the region due to asthenospheric upwelling along the Jemez lineament. U-series dating on travertine also has the potential to provide useful paleohydrologic records across important Quaternary paleoclimate transitions in the Southwest. Groundwater quality is degraded by endogenic fluid mixing. The combined data from springs and travertines such as the La Madera travertine show an interaction of neotectonic and paleoclimatic forces that continue to shape the landscapes, and influence groundwater chemistry, in northern New Mexico.

ACKNOWLEDGMENTS

We thank Bruce Allen and Shari Kelley for thoughtful reviews which improved the manuscript. We thank Dan Koning for his editorial handling and helpful discussion. Support for this work was provided by NSF #EAR/0838575 and NSF#EAR/0719507. We appreciate the permission of the Atterbury family for access to sample sites and wells. We thank Elizabeth Keating for facilitating access to the Chimayo Geyser Well. Water Chemistry was performed in the Analytical Laboratory in the Department of Earth & Planetary Sciences at the University of New Mexico (UNM) with the assistance of Blake Eldridge and Dr. Mehdi Ali. Gas analysis was performed by Dr. David Hilton at Scripps Institute of Oceanography, UCSD, La Jolla, CA and Dr. Richard Poreda at the University of Rochester, Rochester, NY. U-series dating was performed in the Radiogenic Isotope Laboratory at UNM with the assistance of Dr. Yemane Asmerom and Dr. Victor Polyak. This work benefitted from terrace and travertine mapping by the UNM Advanced Field in 2005. Support for A. Tafoya was provided by a Louis Stokes Alliance for Minority Participation Bridge to the Doctorate Fellowship from NSF # EHR/1026412.

REFERENCES

Allen, B.D., 2005, Ice age lakes in New Mexico, New Mexico Museum of Natural History and Science Bulletin , v. 28, p. 107-117

Alonso-Zarza, A.M. and Tanner, L.H., Eds., 2010a, Carbonates in continental settings: Facies, environments and processes, Developments in Sedimentology 61: Elsevier, The Netherlands, 378 p.

Alonso-Zarza, A.M. and Tanner, L.H., eds., 2010b, Carbonates in continental settings: geochemistry, Diagenesis and Applications, Developments in Sedimentology 62: Elsevier, The Netherlands, 319 p.

Asmerom, Y., Polyak, V.J. and Burns, S.J., 2010, Variable winter moisture in the southwestern United States linked to rapid glacial climate shifts: Nature Geoscience, v. 3, p. 114- 117.

Chafetz, H. S., and Folk, R. L., 1984, Travertines: Depositional morphology and the bacterially constructed constituents: Journal of Sedimentary Petrology, v. 54, p. 289-316.

Chiodini, G., Cardellini, C., Amato, A., Boschi, E., Caliro, S., Frondinin, F., and Ventura, G., 2004, Carbon dioxide Earth degassing and seismogenesis in central and southern Italy: Geophysical Research Letters, v. 31, p. 1-4.

Clarke, W.B., Beg, M.A., and Craig, H., 1969, Excess ^3He in the sea; Evidence for terrestrial primordial helium: Earth and Planetary Science Letters, v. 6, p. 213-220.

Craig, H., Lupton, J.E., Welhan, J.A., and Poreda, R.J., 1978, Helium isotopic ratios in Yellowstone and Lassen Park volcanic gases: Geophysical Research Letters, v. 5, p. 897-900.

Craigg, S.W., 1984, Hydrologic data on the Pueblos of Jemez, Zia, and Santa Ana, Sandoval County, New Mexico: United States Geological Survey Open-file Report 84-460, 37 p.

Crossey, L.J., Fischer, T.P., Patchett, P.J., Karlstrom, K.E., Hilton, D.R., Huntoon, P., and Reynolds, A.C., 2006, Dissected hydrologic system at Grand Canyon: Interaction between upper world and lower world waters in modern springs and travertine: Geology, v. 34, p. 25-28.

Crossey, L.J., Karlstrom, K.E., Springer, A., Newell, D., Hilton, D., and Fischer, T., 2009, Degassing of mantle-derived CO_2 and ^3He from springs in the southern Colorado Plateau region— neotectonic connections and implications for groundwater systems: Geological Society of America Bulletin, v. 121, p. 1034-1053. DOI 10.1130/B26394.

Deines, P., Langmuir, D., and Harmon, R.S., 1974, Stable carbon isotope ratios and the existence of a gas phase in the evolution of carbonate ground waters: Geochimica et Cosmochimica Acta, v. 38, p. 1147-1164.

Edwards, R.L., Cheng, H., Murrell, M.T., and Goldstien, S.J., 1997, Protactinium-231 dating of carbonates by thermal ionization mass spectrometry: Implications for Quaternary climate change: Science, v. 276, p. 782-786

Esat, T.M., McCulloch, M.T., Chappell, J., Pillans, B., and Omura, A., 1999, Rapid fluctuations in sea level recorded at Huon Peninsula during the penultimate deglaciation: Science, v. 283, p. 197-209

Fawcett, P.J., Werne, J.P., Anderson, R. S., Jeffery, H.M., Brown, E.T., Berke, M.A., Smith, S.J., Goff, F., Donohoo-Hurley, L., Cisneros-Dozal, L.M., Schouten, S., Sinninghe Damste, J.S., Huang, Y., Toney, J., Fessenden, J., WoldeGabriel, G., Atudorei, V., Geissman, J.W., and Allen, C.D., 2011, Extended megadroughts in the southwestern United States during Pleistocene interglacials: Nature, v. 470, p. 518-521

Formento- Tigilio M.L., and Pazzaglia, F.J., 1998, Tectonic geomorphology of the Sierra Nacimiento: Traditional and new techniques in assessing long-term landscape evolution in the southern Rocky Mountains: Journal of Geology, v. 106, p. 433-454.

Ford, D. C. and Williams, P., 2007, Karst Hydrogeology and Geomorphology:

Wiley and Sons, West Sussex, England. p. 562.
Fouke, B.W., Farmer, J., Des Marais, D., Pratt, L., Sturchio, N., Burns, P. and Discipulo, M., 2000, Depositional facies and aqueous-solid geochemistry of travertine-depositing hot springs (Angel Terrace, Mammoth Hot Springs, Yellowstone National Park, USA): Journal of Sedimentary Research, v. 70, p. 565-585.
Giegengack, R. and Gaines, R., 1979, Havasu Canyon, A natural geochemical laboratory: Proceedings of the First Conference on Scientific Research in the National Parks, v. 2, p. 719-726.
Gilfillan, S.M., Ballentine, C., Holland, G., Blagburn, D., Lollar, B.S., Stevens, S., Schoell, M., and Cassidy, M., 2008, The noble gas geochemistry of natural CO_2 gas reservoirs from the Colorado Plateau and Rocky Mountain provinces, USA: Geochimica et Cosmochimica Acta, v. 72, p. 1174-1198.
Goff, F., 2002, Geothermal potential of Valles Caldera, New Mexico: GHC Bulletin, p. 7-12.
Goff, F., 2009, Valles Caldera: A Geologic History, Albuquerque, University of New Mexico Press, 114 p.
Goff, F. and Gardner, J. N., 1994, Evolution of a mineralized geothermal system, Valles caldera, New Mexico: Economic Geology, v. 89, p. 1803-1832.
Goff, F. and Janik, C. J., 2002, Gas geochemistry of the Valles caldera region, New Mexico and comparisons with gases at Yellowstone, Long Valley and other geothermal systems: Journal of Volcanology and Geothermal Research, v. 116, p. 299-323.
Goff, F. and Shevenell, L. 1987, Travertine deposits of Soda Dam, New Mexico, and their implications for the age and evolution of the Valles caldera hydrothermal system: Geological Society of America Bulletin, v. 99, p. 292-302.
Graham, D.W., 2002, Noble gas isotope geochemistry of mid-ocean ridge and ocean island basalts: Characterization of mantle source reservoirs, *in* Porcelli, D., Ballentine, C.J., and Weiler, R., eds., Reviews in Mineralogy & Geochemistry - Noble Gases in Geochemistry and Cosmochemistry, Volume 47: Washington D.C., Mineralogical Society of America, p. 481-538.
Henderson, G.M. and Slowey, N.C., 2000, Evidence from U–Th dating against Northern Hemisphere forcing of the penultimate deglaciation: Nature, v. 404, p. 61– 66.
Jochems, A.P., Sherson, L.R., Crossey, L.J., and Karlstrom, K.E., 2011, Mixing between an alpine river and hydrothermal spring inputs: Controls on water quality and solute loading in the Jemez River, NM [abstract]: New Mexico Geology, v. 33, p. 59.
Johnson, P.S., Koning, D.J., Timmons, S.W., and Felix, B., 2008, Geochemical characterization of ground water in the southern Espanola Basin, Santa Fe, New Mexico: New Mexico Bureau of Geology Open File Report 511.
Karlstrom, K.E., Crow, R., Peters, L., McIntosh, W., Raucci, J., Crossey, L.J., Umhoefer, P., and Dunbar, N., 2007, $^{40}Ar/^{39}Ar$ and field studies of Quaternary basalts in Grand Canyon and model for carving Grand Canyon: Quantifying the interaction of river incision and normal faulting across the western edge of the Colorado Plateau: Geological Society of America Bulletin, v. 119, p. 1283-1312.
Karlstrom, K.E., Crow, R, Crossey, L.J., Coblentz, D., and van Wijk, J., 2008, Model for tectonically driven incision of the less than 6 Ma Grand Canyon: Geology, v. 36, p. 835-838.
Koning, D.J., Newell, D.L., Sarna-Wojcicki, A., Dunbar, N., Karlstrom, K.E., Salem, A., and Crossey, L.J., 2011, Terrace stratigraphy, ages, and incision rates along the Rio Ojo Caliente, north-central New Mexico: N.M. Geological Society, 62nd Field Conference Guidebook, p. 281-300.
Lisiecki, L.E. and Raymo, M.E., 2005, A Pliocene-Pliestocene stack of 57 globally distributed benthic $\delta^{18}O$ records: Paleoceanography, v. 20, p. 1-17
Lutter, W. J., Roberts, P.M., Thurber, C.H., Steck, L., Fehler, M.C., Stafford, D., Zeichert, T., and Baldridge, S., 1995, Teleseismic P-wave image of the crust and upper mantle structure beneath the Valles caldera, New Mexico: Initial results from the 1993 JTEX passive array, Geophysical Research Letters, v. 22, p. 505-508.
Monroe, S., Antweiler, R., Hart, R., Taylor, H., Truini, M., Rihs, J., and Felger, T., 2005, Chemical characteristics of ground water discharge at selected springs, south rim, Grand Canyon: United States Geologic Survey Scientific Investigations Report 04-5146, 59 p.
Newell, D.L., Crossey, L.J., Karlstrom, K., Fischer, T., and Hilton, D., 2005, Evidence for continental-scale links between the mantle and groundwater systems of the Western United States based on hydrogeochemistry of travertine-depositing springs and regional synthesis of helium isotopic data: GSA Today, v. 15, no. 12, p. 4-10.
Newell, D.L., Jessup, M.J., Cottle, J.M., Hilton, D., Sharp, Z., and Fischer, T., 2008, Aqueous and isotope geochemistry of mineral springs along the southern margin of the Tibetan plateau: Implications for fluid sources and regional degassing of CO_2: Geochemisty, Geophysics, and Geosystems, v. 9, p. Q08014, doi:10.1029/2008GC002021.
Newell, D.L., Koning, D., Karlstrom, K.E., Crossey, L.J., and Dillon, M., 2004, Plio-Pleistocene incision history of the Rio Ojo Caliente, northern Española Basin, and an overview of the Rio Grande system in northern New Mexico: N.M. Geological Society, 55th Field Conference Guidebook, p. 121-134.
O'Nions, R.K., and Oxburgh, E.R., 1988, Helium, volatile fluxes and the development of continental crust: Earth and Planetary Science Letters, v. 90, p. 331-347.
Ozima, M. and Podosek, F., 1983, Noble gas chemistry: Cambridge, United Kingdom, Cambridge Univ. Press, 377 p.
Parkhurst, D.L., 1995, User's guide to PHREEQC—A computer program for speciation, reaction-path, advectivetransport, and inverse geochemical calculations: U.S. Geological Survey Water Resources Investigations Report 95-4227, 143 p.
Pederson, J., and Karlstrom, K.E, 2001, Relating differential incision of Grand Canyon to slip along the Hurricane-Toroweap fault system, *in* Young, R.A., and Spamer, E.E., eds., The Colorado River: Origin and evolution: Grand Canyon, Arizona, Grand Canyon Association Monograph 12, p. 159.166.
Pederson, J.L., Anders, M.D., Rittenhour, T.M., Sharp, W.D., Gosse, J.C., and Karlstrom, K.E., 2006, Using fill terraces to understand incision rates and evolution of the Colorado River in eastern Grand Canyon, Arizona: Journal of Geophysical Research (Earth Surface), v. 111, F02003, doi: 10.1029/2004JF000201
Pederson, J., Karlstrom. K., Sharp, W., and McIntosh, W., 2002, Differential incision of the Grand Canyon related to Quaternary faulting − Constraints from U−series and Ar/Ar Dating: Geology, v. 30, p. 739−742.
Pentecost, A., 1995, The Quaternary travertine deposits of Europe and Asia Minor: Quaternary Science Reviews, v.14, p.1005-1028.
Pentecost, A. , 2005, Travertine: Springer-Verlag Berlin, Berlin, 445 p.
Piper, A.M., 1944, A graphical procedure in the geochemical interpretation of water analyses: Geophysical Union Transactions., v. 25, p. 914-923.
Priewisch, A., Crossey, L.J., Embid, E., Karlstrom, K. E., Polyak, V., Asmerom, Y., and Ricketts, J. 2011, Geochronology, geochemistry and tectonic occurrence of large travertine deposits in New Mexico and Arizona [abstract]: New Mexico Geology, v. 33, no. 2, p. 46-47.
Ray, M.C., Hilton, D.R., Munoz, J., Fischer, T.P., and Shaw, A.M., 2009, The effects of volatile recycling, degassing, and crustal contamination on the helium and carbon geochemistry of hydrothermal fluids from the Southern Volcanic Zone of Chile: Chemical Geology, v. 266, p. 38-49.
Reid, M.R. and Graham, D.W., 1996, Resolving lithospheric and sub-lithospheric contributions to helium isotope variations in basalts from the Southwestern US: Earth and Planetary Science Letters, v. 144, p. 213-222.
Roberts, P. M., Aki, K. and Fehler, M.C. 1995, A shallow attenuating anomaly inside the ring fracture of the Valles caldera, New Mexico: Journal of Volcanology and Geothermal Research, v. 67, p. 79-99.
Rose Coss, Dylan, 2008, Terrace mapping of the Rio Salado and compilation of Quaternary incision rates in northern New Mexico [B.S. Thesis]: University of New Mexico.
Sano, Y., and Marty, B., 1995, Origin of carbon in fumarolic gas from island arcs: Chemical Geology, v. 119, p. 265-274.
Shackleton, N.J., Sanchez-Goni, M.F., Pailler, D., Lancelot, Y., 2003, Marine isotope substage 5e and the Eemian interglacial: Global and Planetary Change, v. 36, p. 151-155
Sower, T., Rose-Cose, D., Karlstrom, K.E., Crossey, L. J., Asmerom, Y., Polyak, V., 2008, Incision history of the Rio Salado and implications for uplift history of the Jemez Mountains [abstract]: New Mexico Geology, v.32, p. 63-64.
Stirling, C., 1998, Timing and duration of the last interglacial: Evidence for a restricted interval of widespread coral reef growth:Earth and Planetary science letters, v. 160, p. 745
Szabo, B., 1990, Ages of travertine deposits in eastern Grand Canyon National Park, Arizona: Quaternary Research, v. 34, p. 24-32.
Tafoya, A.J., Crossey, L.J., Karlstrom, K.K., Kolomaznik, M., Polyak, V., Asmerom, Y., Kelley, S., and Cox, C., 2011, Uranium-series dating of trav-

ertine from Soda Dam, New Mexico: Constructing a history of deposition, with implications for landscape evolution, paleohydrology and paleoclimatology [abstract]: New Mexico Geology v. 33, p. 58.

Turi, B., 1986, Stable isotope geochemistry of travertines, *in* Fritz, P. and Fontes, J.C., eds., The Terrestrial Environment, B. Handbook of Environmental Isotope Geochemistry, Elsevier, Amsterdam, p. 207-238.

Williams, A.J., 2009, An Aqueous Geochemical and Hydrologic Study of the Springs and Wells of the Sevilleta National Wildlife Refuge: Evaluating Hydrochemical Pathways: Albuquerque, New Mexico [M.S. Thesis]: University of New Mexico, 165 p.

Winograd, I.J., Coplen, T.B., Landwehr, J.M., Riggs, A.C., Ludwig, K.R., Szabo, B.J., Kolesar, P.T. and Revesz, K.M., 1992, Continuous 500,000-year climate record from vein calcite in Devils Hole, Nevada: Science, v. 258, p. 255-260.

Woodward, L.A. and Ruetschilling, 1976, Geology of San Ysidro quadrangle, New Mexico: New Mexico Bureau of Mines and Mineral Resources, Geologic Map 37, 1:24,000 scale.

Zeigler, K., Crossey, L., Schuyler, L., Phillips, D., and Karlstrom, K., 2011, Prehistoric Travertine Pendants from Central New Mexico: Potential Relationships with Known Travertine Deposits [abstract]: New Mexico Geology v. 33, p. 57.